Revista Brasileira de Ciências Ambientais
Brazilian Journal of Environmental Sciences

Three-dimensional numerical modeling and analysis of multiphase distribution in a UASB reactor with experimental validation of biogas volumetric flow rate

Modelagem e análise numérica tridimensional da distribuição multifásica em um reator UASB com validação experimental da vazão volumétrica de biogás

Allan Bruno Dantas Gonçalves[1], *Lázaro Nascimento de Freitas*[2], *Maria Gorethe de Sousa Lima Brito*[2], *Flávio César Brito Nunes*[3], *Joelma Pereira da Silva*[2], *Luiz Alberto Ribeiro Mendonça*[2], *Fernando José Araújo da Silva*[1], *Antonio Gilson Barbosa de Lima*[4]

ABSTRACT

Research involving numerical simulations to model physical processes, such as the behavior of multiphase flow in upflow anaerobic sludge blanket (UASB) reactors, requires a validation step for the numerical data to ensure that the model accurately represents the physical dynamics of the studied process. In this context, the present study aimed to develop a mathematical model and perform numerical simulations to investigate the multiphase flow behavior in a UASB reactor, validating the numerical data regarding the biogas volumetric flow rate based on real data collected from the three-phase separator. Using Ansys® CFX software, three-phase, turbulent, transient, Eulerian-Eulerian simulations were conducted with different gas volume fractions (GVF of 0.026; 0.130; and 0.260) at the inlet of the model to examine their influence on phase distribution, velocity, and solid deformation rate. To validate the model, experimental biogas volumetric flow data at the liquid-gas interface were compared with the numerical results, showing a relative error of 4.2% for the case simulated with a GVF of 0.026. In the cases studied, the phase distribution behavior remained consistent. The velocities showed that the gas moved approximately 200 times faster than the liquid, while the solids reached speeds 10 to 30 times higher

RESUMO

Pesquisas envolvendo simulação numérica para modelar processos físicos, como o comportamento do escoamento multifásico em reator anaeróbio de fluxo ascendente e manta de lodo (UASB), requerem uma etapa de validação dos dados numéricos, a fim de assegurar a adequação do modelo para representar a dinâmica física do processo estudado. Neste contexto, esta pesquisa teve como objetivo desenvolver uma modelagem matemática e realizar simulações numéricas para investigar o comportamento do escoamento multifásico em um reator UASB , validando os dados numéricos relativos à vazão volumétrica de biogás por meio de dados reais captados no separador trifásico. Utilizando o software Ansys® CFX, foram simulados casos trifásicos, turbulentos, transientes, Eulerian-Eulerian, considerando diferentes frações volumétricas de gás (FVG de 0,026; 0,130 e 0,260) na entrada do modelo, para investigar sua influência na distribuição e velocidade das fases e na taxa de deformação dos sólidos. Para validação do modelo, dados experimentais da vazão volumétrica de biogás na interface líquido-gás foram comparados com os resultados numéricos, ocorrendo um erro relativo de 4,2% no caso simulado com a FVG de 0,026. Nos casos estudados, o comportamento da distribuição das fases permaneceu constante. As velocidades mostraram que o gás se movia cerca de 200 vezes mais rápido que o líquido, enquanto os sólidos alcançaram velocidades de 10 a 30 vezes superiores às do

[1]Universidade Federal do Ceará – Fortaleza (CE), Brazil.
[2]Universidade Federal de Cariri – Juazeiro do Norte (CE), Brazil.
[3]Instituto Federal de Educação, Ciência e Tecnologia do Ceará – Juazeiro do Norte (CE), Brazil.
[4]Universidade Federal de Campina Grande – Campina Grande (PB), Brazil.

Corresponding author: Allan Bruno Dantas Gonçalves – Federal University of Ceará, Department of Hydraulic and Environmental Engineering, Bl. 713 – CEP: 60451-970 – Fortaleza (CE), Brazil. E-mail: allanbrunoeng@gmail.com

Conflicts of interest: the authors declare no conflicts of interest.

Funding: Coordination for the Improvement of Higher Education Personnel (CAPES) – Funding Code 001; Brazilian National Council for Scientific and Technological Development (CNPq) – Process 406817/2021-9; State Foundation for Scientific and Technological Development Support of Ceará (FUNCAP) Process BP5-0197-00073.02.00/22 and UNI-0210-00652.01.00/23.

Received on: 10/08/2024. Accepted on: 05/15/2025.

https://doi.org/10.5327/Z2176-94782300

than the liquid, but in the opposite direction. It was also found that higher GVF led to increased solid deformation rates due to shear stresses. The validated model is suitable for future studies aiming to improve UASB reactor flow behavior.

Keywords: three-phase flow; computational fluid dynamics; biogas volume fraction; Ansys CFX; sludge deformation rate; phase velocities.

líquido, porém no sentido contrário ao fluxo. Constatou-se ainda que uma maior FVG resulta em uma taxa mais elevada de deformação dos sólidos por tensões de cisalhamento. O modelo validado é adequado para investigações futuras visando melhorias no escoamento de reatores UASB.

Palavras-chave: escoamento trifásico; dinâmica de fluidos computacional; fração volumétrica de biogás; Ansys CFX; taxa de deformação do lodo; velocidade das fases.

Introduction

Upflow anaerobic sludge blanket (UASB) reactors have been a widely used anaerobic technology in recent decades for treating both diluted and concentrated wastewater, especially in tropical climate regions (Lettinga et al., 1980; Souza, 1986; Chong et al., 2012; Mainardis et al., 2020; Kumar et al., 2024). Their applicability extends to a variety of industrial wastewaters, including those from slaughterhouse activities, which are associated with high concentrations of organic matter, solids, oils and greases, pathogens, and nutrients (Lim and Kim, 2014; Bustillo-Lecompte and Mehrvar, 2015, 2016; Loganath and Mazumder, 2018; Musa et al., 2020; Brennan et al., 2021; Gonçalves et al., 2023; Oliveira et al., 2023).

The preference for anaerobic technologies over conventional aerobic ones is attributed to several advantages, e.g., low electricity consumption, low sludge production, the ability to handle high hydraulic and organic loads, reduced nutrient demand, smaller reactor volume, applicability on a small scale, and biogas production with a high methane content (around 50–70%). This last aspect represents an alternative energy source with potential for local use within the wastewater treatment plant itself, for electricity generation, and/or heating purposes (Von Sperling and Chernicharo, 2005; Chernicharo, 2007; Guo et al., 2015; Metcalf and Eddy, 2016; Van Lier et al., 2020; Mpofu et al., 2021). However, these reactors require a post-treatment stage to ensure that the treated wastewater meets environmental standards for discharge or reuse in agriculture, particularly concerning the removal of organic matter, pathogenic microorganisms, and remaining nutrients (Von Sperling and Chernicharo 2005; Lim and Kim, 2014; Metcalf and Eddy, 2016; Daud et al., 2018; Mai et al., 2018). Additionally, rather than being captured in the gas hood, a significant portion of methane (around 50% of total production) is lost as dissolved gas in the effluent. This occurrence can lead to considerable energy losses and contribute to greenhouse gas emissions (Stazi and Tomei, 2021).

It is worth noting that, although desirable from an energy utilization perspective, high methane production in UASB reactors obtained from high volumetric organic loads can significantly alter biochemical reactions. This can adversely impact anaerobic digestion stages, leading to reduced organic matter removal efficiency and decreased methane production (Loganath and Mazumder, 2018; Musa et al., 2019, 2020). Such conditions may also alter the flow regime of fluids and solids. These changes can compromise the stability and operational performance of this type of reactor since its performance also depends on physical factors such as liquid, gas, and solid velocities, interfacial mass transfer, solid integrity, and axial dispersion (Brito et al., 2020).

The various physical factors and their different manifestations within UASB reactors can have a significant impact on their operation, potentially resulting in the development of recirculation zones, solids drag (due to high hydraulic and/or organic loads), gas loss through the reactor's liquid outlet region (fugitive emissions) (Ruttithiwapanich et al., 2013; Das et al., 2018; Brito et al., 2020), and stagnant or poorly mixed zones (in terms of vorticity magnitude) (Vesvikar and Al-Dahhan, 2005; Ren et al., 2008; Cisneros et al., 2021). These factors make the flow dynamics analysis of the reactors quite complex.

As a result, it is crucial to develop methodologies to evaluate flow behavior in these reactors. A viable approach for this study was the use of three-dimensional (3D) numerical simulation through computational fluid dynamics (CFD), which employs pre-defined mathematical models implemented in commercial software capable of simulating complex models on high-performance computers. When combined with experimental data, this methodology allows for the validation of the proposed model and facilitates the analysis of both theoretical and practical operating conditions for this type of reactor.

It should be noted that Brito et al. (2020) and Lima et al. (2011), when studying multiphase flow in UASB reactors treating domestic wastewater in 3D and 2D spaces, respectively, developed a suitable mathematical model to represent the physics of the problem under study. However, the numerical data were validated using suspended solids concentrations at the reactor outlet and pressure distribution along the reactor. Considering this, it is important to assess the possibility of developing a mathematical model and numerical simulation with experimental validation of the numerical data obtained from the biogas volumetric flow rate in the three-phase separator, since this parameter is a key indicator for evaluating the operational performance of UASB reactors.

Bastiani et al. (2021) observed that few studies in literature addressed CFD in the context of three-phase flow. In their review of CFD simulations of granular sludge anaerobic reactors, Bastiani et al. (2023) concluded that a significant knowledge gap remains, particularly the lack of validation of three-phase models with robust experimental data. As the authors pointed out, no documentation exists on the validation of a three-phase model for each phase involved in the flow.

In this scenario, the present study aimed to develop a mathematical model and numerical simulation to investigate the behavior of multiphase flow in UASB reactors in 3D space, with experimental validation of the numerical data for biogas volumetric flow. The primary focus is on the distribution of volumetric phase fractions in the flow as a function of different biogas volume fractions (0.026; 0.130; and 0.260). The proposed steps include: 1. Obtaining experimental data from the monitoring of a UASB reactor used in the treatment of industrial slaughterhouse effluent, which are necessary for specifying the inlet conditions and validating the proposed mathematical model; 2. Verifying whether the dispersed multiphase flow model with interfacial transfer is suitable for modeling the physics of the problem using the Eulerian-Eulerian approach; and 3. Investigating the influence of different biogas volume fractions on the flow of the mixture along the UASB reactor's cross-sectional area, with an emphasis on the analysis of numerical variables, including the velocity and percentage of liquid, solid, and gaseous phases, as well as the deformation rate of the solid phase.

Materials and methods

Numerical simulations of the multiphase flow inside the UASB reactor were performed using the Ansys CFX software.

Three-Dimensional Mesh

The 3D mesh used in this study was developed by Santos Júnior et al. (2017), who produced three distinct meshes with varying element counts (57,008; 96,020; and 184,808 elements). After refinement and dependency analysis, the researchers found that the variations in the results obtained from the three different meshes showed no significant differences.

Based on this finding, the mesh with 57,008 elements was selected to represent the UASB reactor in this study. This choice was grounded in the efficiency of the selected mesh, which, despite having a smaller number of elements than the others, demonstrated the ability to provide reliable results. This efficiency allows for a notable reduction in the computational effort required, optimizing the simulation process.

Figure 1 illustrates the mesh used in this study (A), representing the sludge and three-phase separation regions, with details of the mixture inlet (B), gas outlet (liquid-gas interface) (C), gas deflector (D), liquid outlet (E), and three-phase separator (F). It is important to highlight that the sludge region in the UASB reactor is divided into two main areas: the sludge bed, which extends from the bottom of the reactor to approximately half of its height, and the sludge blanket, which occupies the upper part, from the midpoint up to the deflector.

Multiphase Modeling

In the study of multiphase flow within the UASB reactor, the volume fraction distributions of the three phases—liquid (water), gas (biogas), and solid (sludge)—were analyzed. Following the approach adopted by Brito et al. (2020), the dispersed multiphase flow model with interfacial transfer was selected, using the Eulerian-Eulerian approach.

The consolidation of the multiphase modeling was based on several aspects, including:

- Turbulent and transient flow regime (total time of 50 seconds and timestep of 0.5 seconds).
- Three-phase flow composed of one continuous phase (liquid - α) and two dispersed phases (biogas - β and sludge - γ).
- Biogas was considered a mixture of methane and carbon dioxide in proportions of 75 and 25%, respectively. These proportions were based on experimental data (Gonçalves et al., 2023). The properties of biogas, considered a gas mixture of only methane and carbon dioxide, were determined by calculating the density and molar mass of the mixture (Lima et al., 2011).
- Biogas bubbles and sludge particles were assumed to be spherical with a constant diameter of 3 mm (Owusu-Agyeman et al., 2019; Brito et al., 2020), assuming a homogeneous distribution of biogas bubbles within the cross-sectional area at the reactor inlet (Figure 1B).
- The interfacial momentum transfer between phases α and β was only a function of drag force. According to Chen et al. (2005), drag force has the greatest effect on interfacial momentum transfer models.
- The following coefficients were used to determine drag force: Ishii and Zuber (1979) for the biogas-water fluid pair and Schiller and Naumann (1933) for the water-solid pair.
- The effects of biochemical reactions, temperature variations, and mass transfer between phases were disregarded.
- Due to the complexity involved in studying or modeling porous media, this model did not consider the sludge bed region as a porous medium; instead, it was treated as a free-flow zone to simplify the analysis of the flow within the reactor.

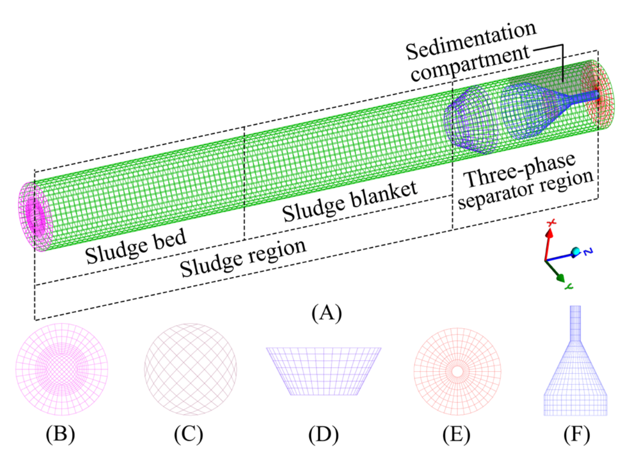

Figure 1 – Illustration of the mesh in three-dimensional space general view (A), highlighting the sludge and three-phase separation regions, mixture inlet (B), gas outlet (C), gas deflector (D), liquid outlet (E), and three-phase separator (F).

Based on the considerations above, the mass conservation equation (Equation 1) and linear momentum equations (Equations 2, 3, and 4) are presented as follows (Brito et al., 2020):

Mass Conservation:

$$\nabla \bullet \left(r_\alpha \rho_\alpha \vec{U}_\alpha\right) = 0 \quad (1)$$

Where:
r_a = volume fraction of phase α;
ρ_a, = density of phase α; and
$\vec{U}_a$ = velocity vector of phase α.

Linear Momentum Conservation:

For the liquid phase:

$$\nabla \bullet \left[r_\alpha\left(\rho_\alpha \vec{U}_\alpha \otimes \vec{U}_\alpha\right)\right] = -r_\alpha \nabla \mathrm{p} + \nabla \bullet \left\{r_\alpha \mu_\alpha \left(\nabla \vec{U}_\alpha + \left(\nabla \vec{U}_\alpha\right)^T\right)\right\} + r_\alpha\left(\rho_\alpha - \rho_{ref}\right) g + c_{\alpha\beta}^{(d)}\left(\vec{U}_\beta - \vec{U}_\alpha\right) \quad (2)$$

Where:
μ_a = dynamic viscosity of phase *a*;
ρ_{ref} = reference density;
g = gravitational force;
$c_{\alpha\beta}^{(d)}$ = interfacial drag term;
T = constant temperature of 29C (isothermal model), and
p = pressure.

For the gas phase:

$$\nabla \bullet \left[r_\beta\left(\rho_\beta \vec{U}_\beta \otimes \vec{U}_\beta\right)\right] = -r_\beta \nabla \mathrm{p} + \nabla \bullet \left\{r_\beta \mu_\beta \left(\nabla \vec{U}_\beta + \left(\nabla \vec{U}_\beta\right)^T\right)\right\} + r_\beta\left(\rho_\beta - \rho_{ref}\right) g + c_{\alpha\beta}^{(d)}\left(\vec{U}_\beta - \vec{U}_\alpha\right) \quad (3)$$

Where:
r_β = volume fraction of phase β;
ρ_β = density of phase β;
$\vec{U}_\beta$ = velocity vector of phase β; and
μ_β = dynamic viscosity of phase β.

For the solid phase:

$$\nabla \bullet \left[r_\gamma\left(\rho_\gamma \vec{U}_\gamma \otimes \vec{U}_\gamma\right)\right] = -r_\gamma \nabla \mathrm{p} + \nabla \bullet \left\{r_\gamma \mu_\gamma \left(\nabla \vec{U}_\gamma + \left(\nabla \vec{U}_\gamma\right)^T\right)\right\} + r_\gamma\left(\rho_\gamma - \rho_{ref}\right) g + c_{\alpha\gamma}^{(d)}\left(\vec{U}_\gamma - \vec{U}_\alpha\right) \quad (4)$$

Where:
Υ_γ = volume fraction of phase γ;
ρ_γ = density of phase γ;
$\vec{U}_\gamma$ = velocity vector of phase γ;
μ_γ = dynamic viscosity of phase γ; and
$c_{\alpha\gamma}^{(d)}$ = interfacial drag term.

Rocha (2017) reports that the k–epsilon model is widely used in turbulence modeling in CFD simulations because it offers an efficient balance between result accuracy and computational effort.

Considering this, terms related to turbulent kinetic energy (Equation 5) and the turbulent dissipation rate (Equation 6) were added to the model in this research (Brito et al., 2020):

Turbulent Kinetic Energy:

$$\nabla \bullet \left\{r_\alpha\left[\rho_\alpha U_\alpha k_\alpha - \left(\mu + \frac{\mu_{t\alpha}}{\sigma_k}\right)\right]\nabla k_\alpha\right\} = r_\alpha\left(P_\alpha - \rho_\alpha \varepsilon_\alpha\right) + T_{\alpha\beta}^{(k)} \quad (5)$$

Where:
K_α = turbulent kinetic energy of phase α;
ε_α = turbulent dissipation rate of phase α;
$\mu_{\tau\alpha}$ = turbulent viscosity of phase α;
$T_{\alpha\beta}^{(k)}$ = interfacial transfer for turbulent kinetic energy;
σ_k = constant with a value of 1.0; and
P_a = turbulence produced due to viscous and buoyant forces.

Turbulent Dissipation Rate:

$$\nabla \bullet \left[r_\alpha \rho_\alpha U_\alpha \varepsilon_\alpha - \left(\mu + \frac{\mu_{t\alpha}}{\sigma_\varepsilon}\right)\nabla \varepsilon_\alpha\right] = r_\alpha \frac{\varepsilon_\alpha}{k_\alpha}\left(C_{\varepsilon 1} P_\alpha - C_{\varepsilon 2} \rho_\alpha \varepsilon_\alpha\right) + T_{\alpha\beta}^{(\varepsilon)} \quad (6)$$

Where:
$T_{\alpha\beta}^{(\varepsilon)}$ = turbulent dissipation rate;
$C_{\varepsilon 1}$ = constant with value of 1.44;
$C_{\varepsilon 2}$ = constant with value of 1.92; and
σ_ε = constant with value of 1.30.

Table 1 details the boundary conditions established for the reactor's 3D mesh. At the gas outlet boundary, which corresponds to the liquid-gas interface, the Degassing condition was applied. This condition allows only the gas phase (biogas bubbles) to pass through. For the liquid (water) and solid (sludge) phases, the condition behaves like a smooth wall, preventing water and sludge from exiting the domain (Ansys, 2024).

The determination of the gas phase volume fraction was based on the estimated biogas production, calculated from the chemical oxygen demand (COD) load entering the reactor, which is converted into methane gas. However, this estimate does not account for the loss of dissolved methane in the effluent, following the methodology proposed by Chernicharo (2007). Furthermore, the calculation of stoichiometric methane production did not consider the total COD of the effluent, but only the biodegradable portion, represented by the biochemical oxygen demand (BOD). Although this approach is not the most commonly used in the literature, it is justified by the fact that the evaluated effluents originate from an industrial slaughterhouse and, unlike domestic sewage, tend to have higher COD concentrations and lower biodegradability (lower BOD), resulting in a high COD/BOD ratio. This choice aims to avoid overestimating biogas production by restricting the estimate to the fraction that is effectively convertible into methane.

Table 1 – Boundary conditions established for the reactor's three-dimensional mesh.

Mesh region	Boundary conditions
Mixture Inlet (Inlet)	Mass and momentum: $U_x = U_y = 0 \; eAu \; U_z = 6e^{-5} \; m.s^{-1}$*
	Turbulence: low (intensity=1%)
Gas Deflector (Wall)	Mass and momentum: No slip wall
Three-Phase Separator (Wall)	Mass and momentum: No slip wall
Reactor Wall (Wall)	Mass and momentum: No slip wall
Gas Outlet (Outlet)	Mass and momentum: Degassing condition
Liquid Outlet (Outlet)	Mass and momentum: Static pressure (Pa): 101,000**

*Established based on the experimental flow rate applied to the reactor (Table 2); **a value of 101,000 Pa was assigned for static pressure at the outlet boundary, corresponding to atmospheric pressure in the municipality of Juazeiro do Norte (CE). A value of 0 Pa was assigned as reference pressure to ensure that absolute pressure at the boundary matched atmospheric pressure (101,000 Pa), since absolute pressure is the sum of static and reference pressures.

The solid volume fraction was calculated based on the production of solids, along with information from specialized literature (Chernicharo, 2007; Brito et al., 2020). The liquid volume fraction was defined to ensure that the sum of the volume fractions of the liquid, solid, and gas phases equaled 1.

The data for the operational conditions, such as hydraulic retention time, flow rate, and environmental parameters inside the reactor (temperature and COD), which are necessary for estimating the gas and solid volume fractions and validating the model, were obtained experimentally (Table 2). It is important to note that substrate collection, system operation, monitoring of the wastewater's physicochemical variables, and determination of biogas volumetric flow rate followed the same methodology used and described by Gonçalves et al. (2023).

By applying the Chernicharo (2007) method to the experimental data gathered in this study to estimate the gas phase volume fraction, a value of 0.026 was obtained (Table 3; case 1). However, to achieve one of the study's objectives, which was to numerically evaluate the reactor's performance at higher gas volume fractions, two additional fractions with higher values were defined (Table 3; cases 2 and 3).

Tables 4 and 5 present the physical properties of the phases analyzed in the study and the numerical methods/convergence criteria adopted, respectively.

For a more detailed discussion of the results, domains were defined along the vertical Zx plane, with levels corresponding to heights of 0.05 m (Z1), 0.58 m (Z2), 0.78 m (Z3), 0.98 m (Z4), and 1.32 m (Z5). These domains allowed for the analysis of the investigated variables (solid deformation rate, velocity, and phase percentages) at various heights of the UASB reactor studied.

Table 2 – Mean values of operating and environmental conditions.

Parameter	Mean value
Temperature (°C)	29
Hydraulic retention time (h)	6.5
Flow rate ($m^3 \cdot s^{-1}$)	$1.03e^{-06}$
Influent COD ($mg \cdot L^{-1}$)	1030.5
Effluent COD ($mg \cdot L^{-1}$)	461.5
Influent BOD ($mg \cdot L^{-1}$)	190.5
Effluent BOD ($mg \cdot L^{-1}$)	108.2
COD/BOD ratio	5.4
Volumetric biogas production ($L \cdot d^{-1}$)	0.72

Table 3 – Volume fractions of the phases at the reactor inlet.

Cases/Phases	Continuous Liquid (water)	Dispersed Gas (biogas)	Dispersed Solid (sludge)
Case 1	0.944	0.026	0.030
Case 2	0.840	0.130	0.030
Case 3	0.710	0.260	0.030

Table 4 – Physical properties of the phases.

Properties	Liquid	Biogas	Solid
Density (ρ: $kg \cdot m^{-3}$)	997	0.72	1020
Dynamic viscosity (μ: $Pa \cdot s$)	$8.899 \cdot 10^{-4}$	$1.114 \cdot 10^{-5}$	$1.295 \cdot 10^{-4}$
Diameter (d: mm)	-	3*	3**
Surface tension (σ: $N \cdot m^{-1}$)	0.072		-

Source: Brito et. al. (2020).

*In accordance with the study by Brito et al. (2020), which adopted an average bubble diameter of 3 mm for bubbles detaching from the bed of a UASB reactor; **Owusu-Agyeman et al. (2019) indicate sludge particle diameters ranging from 0.4 to 4 mm; Metcalf and Eddy (2016) report diameters ranging from 0.5 to 4 mm in UASB reactors; Del Nery et al. (2008) report diameters ranging from 0.5 to 3 mm in a UASB reactor treating poultry slaughterhouse wastewater.

Table 5 – Numerical methods and convergence criteria.

Solver control	
Advection scheme	High resolution
Transient scheme	Second order backward Euler*
Turbulence numerics	High resolution
Convergence criterion	Root mean square residual<1e^{-6}
Convergence control	Minimum loop coefficient: 1
	Maximum loop coefficient: 10**
	Timescale control: Loop coefficient
Interpolation scheme	Pressure: Trilinear
	Velocity: Trilinear
	Geometric shape function

*Recommended for most transient simulations (Ansys, 2024); **for multiphase cases, the standard value of 10 iterations per timestep is more recommended (Ansys, 2024).

Results and discussion

validation of the model

To ensure the reliability and validity of the proposed model, it is essential to perform a comparative analysis between the simulated results and the experimental data. In this context, the biogas volumetric flow rate at the reactor's gas outlet boundary, specifically at the liquid-gas interface, was selected as the parameter for this comparison. The values, detailed in Table 6, provide a clear perspective of this comparison, showing the experimental flow rate, the simulated flow rate, and the relative error.

In Table 6, a variation of 0.03 $L \cdot d^{-1}$ between the numerical and experimental biogas volumetric flow rates is identified, corresponding to a relative error of only 4.2%. This small variation indicates that the applied model effectively represents the multiphase flow inside the UASB reactor.

The low biogas production observed in the UASB reactor under examination can be attributed to the relatively low volumetric organic loading rate (3.81 $kgCOD \cdot m^{-3} \cdot d^{-1}$), which falls within the typical range found in UASB reactors treating domestic effluents (2.5 to 3.5 $kgCOD \cdot m^{-3} \cdot d^{-1}$) (Chernicharo, 2007). These effluents, being significantly more diluted than industrial ones, generate reduced amounts of biogas. Another relevant factor is the COD/BOD ratio of 5.4, indicative of a high inert fraction, which is also considered a limiting factor for biogas production in the reactor studied.

Related research using CFD to investigate the behavior of three-phase flow in UASB reactors has adopted different approaches to model validation. Notably, Lima et al. (2011) and Brito et al. (2020) validated their models by analyzing suspended solids concentration at the reactor outlet in 2D and 3D spaces, respectively, achieving satisfactory results. Similarly, Bastiani et al. (2021), while also examining three-phase flow in UASB reactors, validated their CFD model through numerical simulations, primarily applying the liquid and gas velocity parameters.

Numerical simulations

All numerical simulations were conducted under the same initial and boundary conditions, as specified in Table 3.

Figure 2 illustrates iso-surfaces (vertical plane) in three distinct scenarios, labeled Case 1, Case 2, and Case 3, corresponding to the spatial distribution of the gas volume fraction inside a UASB reactor.

In the three scenarios analyzed, the highest gas volume fraction is observed in the lower part of the reactor, where a constant inlet condition was applied. In this region, the volume fraction of each phase remains at its maximum throughout the simulation. However, due to the difference in density, this fraction changes along the reactor, resulting in a relative decrease in the direction of the flow.

The comparative analysis of the three cases suggests that the distribution of the gas volume fraction, visually observed in Figure 2, is independent of the inlet volume fraction. This finding holds for biogas volume fraction variations between 0.026 and 0.260.

Table 6 – Experimental and numerical biogas volumetric flow rates.

Validation parameters	Case 1
Experimental biogas volumetric flow rate ($L \cdot d^{-1}$)	0.72
Simulated biogas volumetric flow rate ($L \cdot d^{-1}$)	0.75
Relative error (%)	4.2

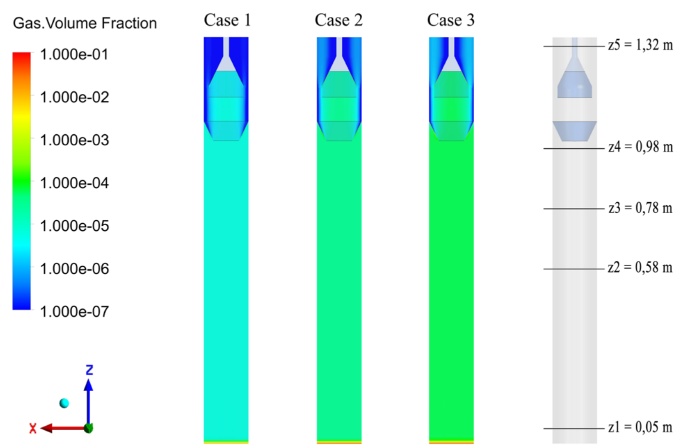

Figure 2 – Iso-surfaces of the gas volume fraction distribution for cases 1, 2, and 3.

Similar behavior was identified in the numerical evaluation conducted by Lima et al. (2011) while investigating the distribution of gas volume fractions. The authors detected significant amounts of biogas along the deflector; however, in their work, the deflector was inclined upward. This configuration facilitated the formation of clustered bubble flows directed towards the interior of the three-phase separator. The authors also noted an almost complete absence of gas entrainment in the sedimentation zone. It is important to highlight that the reactor operated with biogas and sludge fractions of 0.06 and 0.03, respectively.

Regarding the sedimentation compartment, there is no significant presence of gas in the three cases analyzed at elevation Z5 (Table 7). This aligns with practical results and the findings of Lima et al. (2011) and Brito et al. (2020).

Bastiani et al. (2020), while analyzing the vertical profile of the biogas volume fraction distribution generated by the simulation, identified that the gas tended to concentrate primarily near the reactor walls, which reduced the area available for liquid flow. At the top of the reactor, the deflector directed the gas towards the outlet, a behavior that aligns with the observations in this study.

Figure 3 presents three iso-surfaces illustrating the sludge volume fraction in the studied UASB reactor under different flow conditions. The solid volume fractions observed in the upper part of the reactor (three-phase separation region) tend to settle against the phase separator walls. After sedimentation, the solids are directed toward the gas deflector and channeled back into the reactor. This mechanism is crucial for preventing the unwanted loss of solids along with the treated effluent, ensuring that the solids remain inside the reactor. It increases the cell residence time (sludge age), allowing the sludge to continuously participate in the treatment process. Santos et al. (2016) emphasized that reducing the contact time between organic matter and microorganisms in the reactor sludge can compromise the hydrolysis of biodegradable COD and its conversion into soluble substrate, which, in subsequent stages, is transformed into methane.

Table 8 shows that the gas velocity reaches approximately 200 times the liquid velocity, primarily due to buoyancy effects. On the other hand, solids' velocity, which moves in the opposite direction, is about 10 to 30 times that of the liquid and is mainly driven by gravity. According to Das et al. (2018), biogas bubbles rise with the turbulence of the flow upon detachment from the sludge bed. This movement leads to an upward flow velocity of the mixture higher than that generated by the liquid alone. These results also indicate that the interfacial transfer model used in this research is physically suitable for representing the problem, as each fluid has its own velocity field while sharing the same pressure field.

Table 9 details the values obtained for the sludge deformation rate in domains Z1 to Z5 for the different cases studied.

Table 9 shows that, as the inlet gas volume fraction increases, the solid deformation rate in domains Z1, Z2, and Z3 also increases. This deformation increase can be attributed to the shear stress between the rising bubbles and the descending solids. This trend becomes clear when comparing cases 1, 2, and 3.

Domain Z4 showed random results, which can be linked to its proximity to the gas deflector, making this region particularly complex for evaluation. This complexity may be related to the water recirculation caused by the reduction in the section area diameter.

In domain Z5, significantly lower deformation stresses were recorded compared to the other domains. This finding can be attributed to the absence of biogas bubbles in this domain, as shown in Table 7. Therefore, the solid deformation stress in this specific region is solely attributed to the upward liquid flow acting on the counterflowing solid particles.

Another relevant finding concerns the percentage of solids distributed within the UASB reactor (Table 7). In the different cases studied, the percentage of solids in domain Z5 was approximately 3.5%. Conversely, in domains Z2, Z3, and Z4, across all three cases, the percentage values ranged from 2.0 to 2.7%.

The average upward water velocities were 0.0008 $m \cdot s^{-1}$ for cases 1, 2, and 3 at Z2 (0.58 m). Z2 is a height at which the flow behavior is expected to be representative of the digestion compartment (corresponding to the sludge bed; Figure 1), regardless of the inlet boundary conditions or the gas deflector. These velocities exceeded the maximum values established by Brazilian Regulatory Standard NBR 12.209/2011 (Design of hydraulic-sanitary systems for wastewater treatment plants), which are as follows: 0.000194 $m \cdot s^{-1}$ for average flow and 0.000333 $m \cdot s^{-1}$ for peak flow (ABNT, 2011). The average surface flow rate in the settling compartment also exceeded the values specified by the standard. These results indicate that sludge particle carryover occurred from the sludge zone to the settling compartment, resulting in an increased solids concentration in this compartment (specifically at Z5).

The lower percentage values in Z2, Z3, and Z4 are associated with the fact that these domains are located in the sludge region, where the flow is shared among the three phases (liquid, solids, and gas), unlike domain Z5, which is part of the sedimentation compartment. In this compartment, solids transported to the top of the reactor tend to return to the sludge blanket due to gravity, resulting in a biphasic (liquid–solid) separation. Theoretically, the domain Z5 should be a region predominantly characterized by liquid flow.

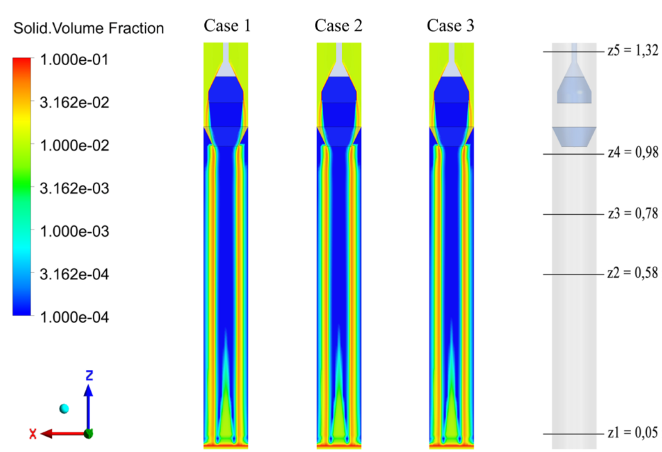

Figure 3 – Iso-surfaces of the sludge volume fraction distribution for cases 1, 2, and 3.

Table 7 – Percentage of phases at different reactor heights.

Cases	Liquid phase (%)			Solid phase (%)			Gas phase (%)		
	1	2	3	1	2	3	1	2	3
Z1: 0.05 m	49.741	50.496	51.145	50.258	49.498	48.844	0.001	0.006	0.011
Z2: 0.58 m	97.329	97.329	97.327	2.671	2.668	2.666	0.001	0.003	0.007
Z3: 0.78 m	97.313	97.312	97.310	2.686	2.685	2.683	0.001	0.003	0.007
Z4: 0.98 m	97.915	97.906	97.867	2.085	2.091	2.127	0.001	0.003	0.006
Z5: 1.32 m	96.504	96.507	96.512	3.496	3.492	3.488	0.000	0.000	0.000

Table 8 – Phase velocities at different reactor heights.

Velocities	Liquid (m·s⁻¹)			Solid (m·s⁻¹)			Gas (m·s⁻¹)		
Cases	1	2	3	1	2	3	1	2	3
Z1	0.0069	0.0071	0.0073	-0.0120	-0.0119	-0.0118	0.1260	0.1262	0.1266
Z2	0.0008	0.0008	0.0008	-0.0272	-0.0273	-0.0273	0.2298	0.2298	0.2297
Z3	0.0009	0.0008	0.0008	-0.0272	-0.0273	-0.0273	0.2298	0.2298	0.2298
Z4	0.0011	0.0011	0.0011	-0.0257	-0.0247	-0.0267	0.2303	0.2303	0.2302
Z5	0.0010	0.0010	0.0010	-0.0269	-0.0269	-0.0269	0.2051	0.2246	0.2275

Table 9 – Solid deformation rate at different reactor heights.

Solid deformation rate (s^{-1})			
Cases	1	2	3
Z1: 0.05 m	0.5662	0.5735	0.5824
Z2: 0.58 m	0.5871	0.5876	0.5887
Z3: 0.78 m	0.6250	0.6258	0.6285
Z4: 0.98 m	1.1552	1.2460	0.9888
Z5: 1.32 m	0.2174	0.2147	0.2115

In domains 2 (Z2=0.58 m), 3 (Z3=0.78 m), and 4 (Z4=0.98 m), the solids percentages were found to be consistent with those typically observed in the operation of UASB reactors, which, according to Chernicharo (2007), generally range between 1 and 3%. However, these values exceed the maximum safety limit recommended by Lobato et al. (2018), which is 0.5%, in order to prevent sludge carryover to the sedimentation compartment and excessive solids loss in the effluent. To meet the recommendation of Lobato et al. (2018), considering the current reactor configuration and the same solid characteristics, it would be necessary to reduce the upward liquid velocity in the inlet domain of the reactor.

Figure 4 illustrates three distinct representations of the water volume fraction in the studied UASB reactor.

In Figure 4, the predominance of red coloration reflects the high liquid volume fraction. However, the formation of blue trails indicates the path of settling solids, a feature similar to that observed in Figure 3 for the solid volume fraction.

In all three scenarios, the blue trails outlining the sludge sedimentation path remain consistent, despite variations in water and biogas volume fractions. These trails provide insights into the flow behavior and sludge retention. The visual similarities reinforce the understanding that changes in the water and biogas volume fractions do not directly affect the sludge sedimentation pattern.

Bastiani et al. (2021) reported that water flow occurs through the central part of the reactor, influenced by the tendency of biogas to concentrate mainly near the reactor walls. This phenomenon may be related to the distribution system used by the authors.

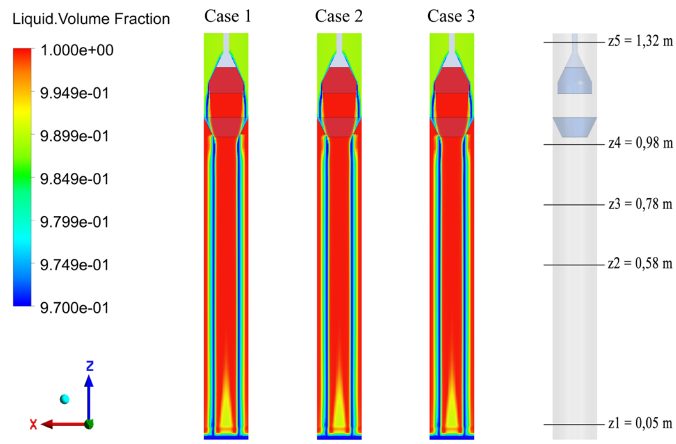

Figure 4 – Iso-surfaces of the water volume fraction distribution for cases 1, 2, and 3.

Conclusions

The validation of the mathematical modeling of multiphase flow in a 3D UASB reactor used in this research was considered adequate, as the discrepancy between the numerically obtained biogas volumetric flow rate and the experimental measurement was 0.3 $L \cdot d^{-1}$, representing a relative error of only 4.2%.

The dispersed multiphase flow model with interfacial transfer, using the Eulerian-Eulerian approach, also proved physically suitable for representing the investigated problem, as each phase of the liquid, solid, and gas mixture exhibited distinct velocity fields.

The results indicated that the flow behavior of the liquid, solid, and gas phases remained constant, regardless of the inlet gas volume fraction. The difference in velocities between gas and solids, governed by buoyancy and gravity, respectively, was also highlighted, with gas moving approximately 200 times faster than the liquid, while solids moved 10 to 30 times faster than the liquid in the opposite direction.

It was also observed that an increase in the gas volumetric fraction at the reactor inlet results in a higher deformation rate of solids during the sedimentation process in the sludge region.

It is important to emphasize that for the modeling to be applicable to larger-scale reactors, it is essential to consider how changes in reactor dimensions will affect the overall system performance. This requires a detailed assessment of hydrodynamic conditions, including the analysis of velocities, volumetric fractions, shear rates, and other relevant parameters, to ensure that the model adequately represents the flow behavior at a larger scale.

The lack of previous research using CFD in UASB reactor multiphase flows, which validates its modeling based on biogas volumetric flow rate, underscores the innovative nature of this study. This approach offers a new validation criterion that could guide future research in UASB reactor flow modeling.

Authors' Contributions

Gonçalves, A.B.D: conceptualization, data curation, formal analysis, data acquisition, investigation, methodology, software, validation, visualization, writing – original draft, writing – review and editing. **Freitas**, L.N.: conceptualization, data curation, formal analysis, data acquisition, investigation, methodology, software, validation, visualization, writing – original draft. **Brito**, M.G.S.L.: data curation, formal analysis, funding acquisition, data acquisition, investigation, methodology, project administration, resources, software, supervision, validation, visualization, writing – original draft, writing – review and editing. **Nunes**, F.C.N.: conceptualization, data curation, formal analysis, data acquisition, funding acquisition, software, writing – review and editing. **Silva**, J.P: data curation, formal analysis, data acquisition, investigation, writing – original draft. **Mendonça**, L.A.R.: conceptualization, data curation, formal analysis, writing – review and editing. **Silva**, F.J.A.: data curation, formal analysis, investigation, methodology, supervision, validation, visualization, writing – review and editing. **Lima**, A.G.B.: formal analysis, investigation, methodology, writing – review and editing.

References

Ansys, 2024. Ansys CFX-Solver Modeling Guide.

Associação Brasileira de Normas Técnicas (ABNT), 2011. NBR 12209: Elaboração de projetos hidráulico-sanitários de estações de tratamento de esgotos sanitários. 2. ed. ABNT, Rio de Janeiro.

Bastiani, C.D'; Alba, J.L.; Mazzarotto, G.T.; Farias Neto, S.R.; Reynolds, A.; Kennedy, D.; Beal, L.L., 2021. Three-phase hydrodynamic simulation and experimental validation of an upflow anaerobic sludge blanket reactor. Computers & Mathematics with Applications, v. 83, 95-110. https://doi.org/10.1016/j.camwa.2020.02.017.

Bastiani, C.D'; Alba, J.L.; Mazzarotto, G.T.; Farias Neto, S.R.; Torres, A.P.R.; Beal, L.L., 2020. CFD simulation and piv validation of the gas/liquid behavior in an uasb reactor. Engenharia Sanitária e Ambiental, v. 25 (1), 87-96. https://doi.org/10.1590/s1413-41522020179462.

Bastiani, C.D'; Ken, D.; Reynolds, A., 2023. CFD simulation of anaerobic granular sludge reactors: a review. Water Research, v. 242, 120220. https://doi.org/10.1016/j.watres.2023.120220.

Brennan, B.; Gunes, B.; Jacobs, M.R.; Lawler, J.; Regan, F., 2021. Potential viable products identified from characterisation of agricultural slaughterhouse rendering wastewater. Water, v. 13 (3), 352. https://doi.org/10.3390/w13030352.

Brito, M.G.S.L.; Nunes, F.C.B.; Magalhães, H.L.F.; Lima, W.M.P.B.; Moura, F.L.C.; Farias Neto, S.R.; Lima, A.G.B., 2020. Hydrodynamics of uasb reactor treating domestic wastewater: a three-dimensional numerical study. Water, v. 12 (1), 279. https://doi.org/10.3390/w12010279.

Bustillo-Lecompte, C.F.; Mehrvar, M., 2015. Slaughterhouse wastewater characteristics, treatment, and management in the meat processing industry: A review on trends and advances. Journal of Environmental Management, v. 161, 287-302. https://doi.org/10.1016/j.jenvman.2015.07.008.

Bustillo-Lecompte, C.F.; Mehrvar, M., 2016. Treatment of an actual slaughterhouse wastewater by integration of biological and advanced oxidation processes: modeling, optimization, and cost-effectiveness analysis. Journal of Environmental Management, v. 182, 651-666. https://doi.org/https://doi.org/10.1016/j.jenvman.2016.07.044.

Chen, P.; Sanyal, J.; Duduković, M.P., 2005. Numerical simulation of bubble columns flows: effect of different breakup and coalescence closures. Chemical Engineering Science, v. 60 (4), 1085-1101. https://doi.org/10.1016/j.ces.2004.09.070.

Chernicharo, C.A.L., 2007. Anaerobic Reactors. IWA Publishing, London. https://doi.org/10.2166/9781780402116.

Chong, S.; Sen, T.K.; Kayaalp, A.; Ang, H.M., 2012. The performance enhancements of upflow anaerobic sludge blanket (uasb) reactors for domestic sludge treatment – a state-of-the-art review. Water Research, v. 46 (11), 3434-3470. https://doi.org/10.1016/j.watres.2012.03.066.

Cisneros, J.F.; Cobos, F.; Pelaez-Samaniego, M.R.; Rehman, U.; Nopens, I.; Alvarado, A., 2021. Hydrodynamic evaluation of five influent distribution systems in a cylindrical uasb reactor using cfd simulations. Water, v. 13 (21), 3141. https://doi.org/10.3390/w13213141.

Das, S.; Sarkar, S.; Chaudhari, S., 2018. Modification of uasb reactor by using cfd simulations for enhanced treatment of municipal sewage. Water Science and Technology, v. 77 (3), 766-776. https://doi.org/10.2166/wst.2017.584.

Daud, M.K.; Rizvi, H.; Akram, M.F.; Ali, S.; Rizwan, M.; Nafees, M.; Jin, Z.S., 2018. Review of upflow anaerobic sludge blanket reactor technology: effect of different parameters and developments for domestic wastewater treatment. Journal of Chemistry, v. 2018, 1-13. https://doi.org/10.1155/2018/1596319.

Gonçalves, A.B.D.; Brito, M.G.S L.; Nunes, F.C.B.; Silva, F.J.A.; Silva, J.P.; Oliveira, C.G., 2023. Efeito da configuração do separador de fases na captação de biogás em reatores uasb tratando águas residuárias de frigorífico industrial. Ciência e Sustentabilidade, v. 7 (1), 322-360. https://doi.org/10.56837/ces.v7i01.1132.

Guo, M.; Song, W.; Buhain, J., 2015. Bioenergy and biofuels: history, status, and perspective. Renewable and Sustainable Energy Reviews, v. 42, 712-725. https://doi.org/https://doi.org/10.1016/j.rser.2014.10.013.

Ishii, M.; Zuber, N., 1979. Drag coefficient and relative velocity in bubbly, droplet or particulate flows. AIChE Journal, v. 25 (5), 843-55. https://doi.org/10.1002/aic.690250513.

Kumar V, K.; Mahendiran, R.; Subramanian, P.; Karthikeyan, S., 2024. Upflow anaerobic sludge blanket (uasb) reactors for bio-methane production from limed tannery fleshings: lab and pilot scale reactors. Sustainable Chemistry One World, v. 2, 100006. https://doi.org/10.1016/j.scowo.2024.100006.

Lettinga, G.; Van Velsen, A.F.M.; Hobma, S.W.; Zeeuw, W.; Klapwijk, A., 1980. Use of the upflow sludge blanket (usb) reactor concept for biological wastewater treatment, especially for anaerobic treatment. Biotechnology and Bioengineering, v. 22 (4), 699-734. https://doi.org/10.1002/bit.260220402.

Lim, S.J.; Kim, T., 2014. Applicability and trends of anaerobic granular sludge treatment processes. Biomass and Bioenergy, v. 60, 189-202. https://doi.org/10.1016/j.biombioe.2013.11.011.

Lima, M.G.S.; Farias Neto, S.R.; Lima, A.G.B.; Nunes, F.C.B.; Gomes, L.A., 2011. Theoretical/experimental study of an upflow anaerobic sludge blanket reactor treating domestic wastewater. International Journal of Chemical Reactor Engineering, v. 9, (1). https://doi.org/10.1515/1542-6580.2599.

Lobato, L.C.S.; Bressani-Ribeiro, T.; Silva, B.S.; Flórez, C.A.D.; Neves, P.N.P.; Chernicharo, C.A.L., 2018. Contribuição para o aprimoramento de projeto, construção e operação de reatores UASB aplicados ao tratamento de esgoto sanitário. Parte 3: Gerenciamento de lodo e escuma. Sabesp: Revista DAE, v. 66, (214), 30-55. https://doi.org/10.4322/dae.2018.040.

Loganath, R.; Mazumder, D., 2018. Performance study on organic carbon, total nitrogen, suspended solids removal and biogas production in hybrid UASB reactor treating real slaughterhouse wastewater. Journal of Environmental Chemical Engineering, v. 6, (2), 3474-3484. https://doi.org/10.1016/j.jece.2018.05.031.

Mai, D.T.; Kunacheva, C.; Stuckey, D.C., 2018. A review of posttreatment technologies for anaerobic effluents for discharge and recycling of wastewater. Critical Reviews in Environmental Science and Technology, v. 48 (2), 167-209. https://doi.org/10.1080/10643389.2018.1443667.

Mainardis, M.; Buttazzoni, M.; Goi, D., 2020. Up-flow anaerobic sludge blanket (uasb) technology for energy recovery: a review on state-of-the-art and recent technological advances. Bioengineering, v. 7 (2), 43. https://doi.org/10.3390/bioengineering7020043.

Metcalf, L.; Eddy, H.P., 2016. Tratamento de efluentes e recuperação de recursos. AMGH, Porto Alegre.

Mpofu, A.B.; Oyekola, O.O.; Welz, P.J., 2021. Anaerobic treatment of tannery wastewater in the context of a circular bioeconomy for developing countries. Journal of Cleaner Production, v. 296, 126490. https://doi.org/10.1016/j.jclepro.2021.126490.

Musa, M.A.; Idrus, S.; Harun, M.R.; Marzuki, T.F.T.M.; Wahab, A.M.A., 2020. A comparative study of biogas production from cattle slaughterhouse wastewater using conventional and modified upflow anaerobic sludge blanket (uasb) reactors. International Journal of Environmental Research and Public Health, v. 17 (1), 283. https://doi.org/10.3390/ijerph17010283.

Musa, M.A.; Idrus, S.; Man, H.C.; Daud, N.N.N., 2019. Performance comparison of conventional and modified upflow anaerobic sludge blanket (uasb) reactors treating high-strength cattle slaughterhouse wastewater. Water, v. 11 (4), 806. https://doi.org/10.3390/w11040806.

Nery, V.D.; Pozzi, E.; Damianovic, M.H.R.Z.; Domingues, M.R.; Zaiat, M., 2008. Granules characteristics in the vertical profile of a full-scale upflow anaerobic sludge blanket reactor treating poultry slaughterhouse wastewater. Bioresource Technology, v. 99 (6), 2018-2024. https://doi.org/10.1016/j.biortech.2007.03.019.

Oliveira, T.D.; Nepomuceno, D.C.F.; Naval, L.P., 2023. Reuse of Effluents from Cattle Slaughterhouses: Multicriteria Evaluation. Revista Brasileira de Ciências Ambientais, v. 58 (2), 203-211. https://doi.org/10.5327/Z2176-94781624.

Owusu-Agyeman, I.; Özge, E.; Cetecioglu, Z; Plaza, E., 2019. the study of structure of anaerobic granules and methane producing pathways of pilot-scale uasb reactors treating municipal wastewater under sub-mesophilic conditions. Bioresource Technology, v. 290, 121733. https://doi.org/10.1016/j.biortech.2019.121733.

Ren, T.; Mu, Y.; Ni, B.; Yu, H., 2009. Hydrodynamics of upflow anaerobic sludge blanket reactors. AIChE Journal, v. 55 (2), 516-528. https://doi.org/10.1002/aic.11667.

Rocha, V. C., 2017. Modelagem hidro-bioquímica de reatores anaeróbios: aplicação da dinâmica de fluidos computacional e da dinâmica de sistemas. Doctoral Thesis, Escola de Engenharia de São Carlos, Universidade de São Paulo, São Paulo. doi: 10.11606/T.18.2017.tde-20062017-103746. Retrieved 2024-02-02 from www.teses.usp.br

Ruttithiwapanich, T.; Songkasiri, W.; Ruenglertpanyakul, W., 2013. Identification of granular sludge wash-out origin inside an upflow industrial-scale biogas reactor by the three-phase flow model. IERI Procedia, v. 5, 245-251. https://doi.org/10.1016/j.ieri.2013.11.099.

Santos Júnior, F.N.; Rodrigues, R.O.; Nunes, F.C.B., 2017. Hidrodinâmica em um reator uasb convencional e tipo y tratando água residuária doméstica: um estudo numérico tridimensional. In Anais SEMIC. PRPI, Juazeiro do Norte.

Santos, S.L.; Chaves, S.R.M.; Van Haandel, A., 2016. Influence of phase separator design on the performance of uasb reactors treating municipal wastewater. Water SA, v. 42 (2), 176-182. https://doi.org/10.4314/wsa.v42i2.01.

Schiller, L.; Naumann, Z., 1933. Über die grundlegenden berechungen bei der schwerkraftbereitung. Zeitschrift Des Vereins Deutscher Ingenieure, v. 77, 318-320.

Souza, M.E., 1986. Criteria for the utilization, design and operation of uasb reactors. Water Science and Technology, v. 18 (12), 55-69. https://doi.org/10.2166/wst.1986.0163.

Stazi, V.; Tomei, M.C., 2021. Dissolved methane in anaerobic effluents: a review on sustainable strategies for optimization of energy recovery or internal process reuse. Journal of Cleaner Production, v. 317, 128359. https://doi.org/10.1016/j.jclepro.2021.128359.

Van Lier, J.B.; Mahmoud, N.; Zeeman, G., 2020. Anaerobic wastewater treatment. In: Chen, G.; van Loosdrecht, M.C.M.; Ekama, G.A.; Brdjanovic D. (Eds), Biological wastewater treatment: principles, modeling and design. IWA Publishing, London, pp. 701-756. https://doi.org/10.2166/9781789060362_0701.

Vesvikar, M.S.; Al-Dahhan, M., 2005. Flow pattern visualization in a mimic anaerobic digester using CFD. Biotechnology and Bioengineering, v. 89 (6), 719-732. https://doi.org/10.1002/bit.20388.

Von Sperling, M.; Chernicharo, C.A.L., 2005. Biological wastewater treatment in warm climate regions. London, IWA Publishing.